

Preclinical Cancer Imaging

Ravinder Reddy, PhD. krr@upenn.edu

Center for Magnetic Resonance and Optical Imaging, Department of Radiology, University of Pennsylvania, B1 Stellar-Chance Labs, 422 Curie Boulevard, Philadelphia, PA 19104

Highlights

- Chemical Exchange Saturation Transfer (CEST) based Magnetic Resonance Imaging (MRI) methods inherently have superior sensitivity to molecular changes in tumors.
- CEST MRI provides unconventional and in many cases molecular specific image contrast. CEST contrast can be turned on and off.
- CEST MRI is sensitive to pH and molecular changes in tumors.
- It enables the differential diagnosis between radiation necrosis and tumor recurrence.
- It enables high resolution imaging of glucose metabolism and protease activity in cancer.
- It has the potential to serve as an imaging biomarker for diagnosis of tumors and monitoring tumor response to therapy.

Talk Title: Chemical Exchange Saturation Transfer (CEST) Imaging of Cancer

Target Audience: Students, post doctoral fellows, research investigators in the fields of MR physics, Biophysics, Radiology and Oncology who have an interest in learning about novel imaging biomarkers for diagnosis and monitoring of tumor response to therapy.

Objectives: Learners will be able to grasp basic principles and technical aspects of CEST MRI described in this talk and apply them in their current ongoing research to enhance the capability to image a range of metabolic changes in different types of tumors.

Purpose: The primary purpose of this talk is to impart basic principle of CEST, including theoretical background, experimental details, and show some exciting applications of the method in imaging cancer to elicit information that is not available from other imaging modalities. In addition, describe potential advantages and limitations of the methods in implementing both in preclinical and clinical imaging.

Methods

Background: Chemical exchange processes and their effects on the Nuclear Magnetic Resonance (NMR) spectrum were some of the main topics of investigation that led to several key advancements in the early days of NMR^{1,2}. However, only recently have these processes been exploited for contrast on MRI through saturation transfer experiments³. CEST is a new contrast enhancement technique that enables the indirect detection of molecules with exchangeable protons and exchange-related properties^{4,5}. CEST makes MRI sensitive to the concentrations of endogenous metabolites and their environments.

CEST agents, molecules with exchangeable protons, can be divided into two classes: (i) paramagnetic CEST agents (PARACEST) and (ii) diamagnetic CEST agents. Molecules with exchangeable protons capable of providing CEST contrast combined with a paramagnetic metal ion (typically one of the lanthanides) are known as PARACEST agents. On the other hand, diamagnetic CEST agents are simply molecules with exchangeable protons without

paramagnetic ions. PARACEST agents create larger chemical shifts between exchangeable protons, which allow for more selective irradiation and imaging of faster exchanging species⁶⁻⁸. While these PARACEST agents have promising applications, a detailed discussion of these is beyond the scope of this lecture. The reader is referred to several excellent reviews summarizing the PARACEST literature⁹⁻¹¹.

This presentation focuses on the recent developments in diamagnetic CEST methods and their potential applications in cancer imaging. Briefly, we outline the principle and theoretical aspects of CEST and review recent developments in CEST MRI from amides on proteins, amine groups on small metabolites such as glutamate (Glu), and hydroxyl groups on glucose. Potential applications of amide, amine and -OH CEST in imaging aspects of cancer will be illustrated with some compelling examples. Finally, strengths and some of the limitations of CEST imaging are outlined. For a thorough discussion of theoretical aspects and in depth review of CEST applications, the reader is referred to several outstanding reviews^{10,12-15} on this topic.

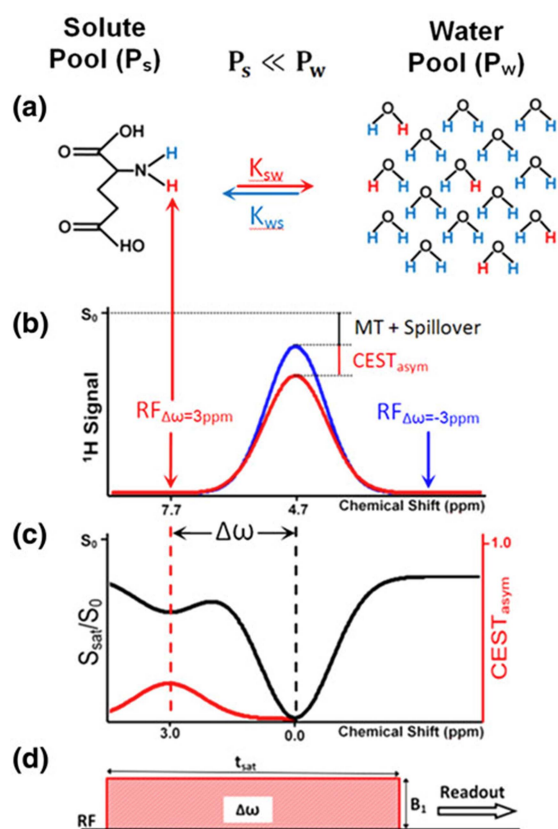


Figure 1: CEST contrast enhancement mechanism illustrated with a two-site exchange between a solute pool and a solvent pool (water). **(a)** Radiofrequency (RF) saturation applied at the resonance frequency ($\Delta\omega$) of the labile solute protons (P_s) leads to a loss of net magnetization. These saturated protons (red) from the solute pool then exchange with unsaturated protons (blue) from the much larger water pool (P_w) with an exchange rate, k_{sw} leading to an accumulation of saturated protons in the water pool. **(b)** The accumulation of the zero net magnetization of solute protons in water results in a decrease in the total water signal. While the saturation pulse is being applied, this process continues to decrease the water magnetization through the CEST effect as well as through magnetization transfer (MT) and direct water saturation or “spillover” effects. A saturation pulse applied at the corresponding reference frequency symmetrically at the opposite side of the water resonance ($-\Delta\omega$) will decrease the water magnetization through MT and spillover effects only. **(c)** Saturation transfer effects can be assessed using a z-spectrum (black curve) where the water signal is plotted as a function of saturation frequency. Here the water resonance frequency is used as the center frequency and assigned the chemical shift of 0 ppm as opposed to in NMR spectra, where water protons have a chemical shift of 4.7 ppm. Asymmetry analysis ($CEST_{asym}$) is performed by subtracting the water signal from one side of the z-spectrum from the other side to mitigate the effects of spillover as well MT effects and isolate the effects of chemical exchange. **(d)** Standard CEST magnetization preparation consisting of a long saturation pulse applied at a resonance frequency, $\Delta\omega$, at a saturation amplitude, B_1 , and duration t_{sat} . The saturation pulse can be a single, long frequency selective rectangular pulse, as shown here or a train of shaped frequency selective pulses separated by small delays¹²

from one side of the z-spectrum from the other side to mitigate the effects of spillover as well MT effects and isolate the effects of chemical exchange. **(d)** Standard CEST magnetization preparation consisting of a long saturation pulse applied at a resonance frequency, $\Delta\omega$, at a saturation amplitude, B_1 , and duration t_{sat} . The saturation pulse can be a single, long frequency selective rectangular pulse, as shown here or a train of shaped frequency selective pulses separated by small delays¹²

Theory of CEST: Let us consider a two-site exchange process involving a solute pool (P_s) with exchangeable protons and a much larger solvent (water) pool (P_w). In CEST imaging, a frequency selective radiofrequency (RF) saturation pulse is applied to the solute pool (figure 1d). A long saturation pulse applied at the resonance frequency of the solute protons, equalizes the number of spins aligned against the magnetic field to those aligned with the magnetic field

leading to no net magnetization and result in the process termed “saturation”, the net result of which is zero MR signal. This zero magnetization of saturated protons from the solute pool then exchanges with unsaturated protons from the much larger water pool leading to decrease in the water signal proportional to the concentration of solute (figure 1a). While the saturation pulse is being applied, this process continues to decrease the water magnetization, which may be viewed as a negative “hyperpolarization of water pool”. Concurrently, longitudinal relaxation processes return the saturated proton spins to their thermal equilibrium state until the system reaches steady state or the saturation pulse is turned off. The reduction in the water signal can be imaged with any routine imaging sequences. The cumulative saturation of water magnetization (akin to negative “hyperpolarization of water pool”) during the saturation period is responsible for the enhanced sensitivity of CEST MRI in detecting solute pool signal.

CEST contrast requires that a discrete chemical shift difference ($\Delta\omega$) between water and the exchangeable proton on the solute is preserved, and the exchange rate, k_{sw} , has to fulfill the slow to intermediate exchange condition on the NMR time scale defined as ¹⁶

$$k_{sw} \leq \Delta\omega \quad [1]$$

Generally, the saturation pulses are not perfectly frequency selective and therefore lead to some direct saturation of the water protons or “spillover” effects (figure 1b). Additionally, in biological tissues, the saturation of solute pools also causes magnetization transfer (MT) between water molecules bound to larger macromolecules in solid or semisolid phases and free water protons, which also leads to a decrease in the water signal. These different saturation transfer effects can be assessed using a z-spectrum generated by plotting the water signal as a function of saturation frequency. Since the direct water saturation effects are symmetric with respect to the water resonance frequency, they can be removed by asymmetry analysis where the water signal from one side of the z-spectrum is subtracted from the other side¹⁵ (figure 1c). Under certain saturation parameters, asymmetry analysis will also remove the contribution of MT. Thus, to isolate the chemical exchange effects of a particular metabolite, the CEST asymmetry ratio (CEST_{asym}) is computed by subtracting the normalized magnetization signal at the exchangeable solute proton frequency [$M_{sat}(+\Delta\omega)$] where $\Delta\omega$ is the chemical shift difference between solute and labile protons, from magnetization at the corresponding reference frequency symmetrically at the opposite side of the water resonance [$M_{sat}(-\Delta\omega)$]:

$$\text{CEST}_{\text{asym}} = \frac{M_{\text{sat}}(-\Delta\omega) - M_{\text{sat}}(+\Delta\omega)}{M_{\text{ctl}}} \quad [2]$$

where M_{ctl} is the control magnetization. For M_{ctl} , either M_0 , the magnetization observed with no saturation, the magnetization observed with a saturation pulse far from the water resonance (≥ 20 ppm), or the $M_{\text{sat}}(-\Delta\omega)$ magnetization can be used¹⁷. In interpreting the CEST effect, factors that play a role are the concentration of the solute, the proton exchange rate, the number of exchangeable protons, the pH of the local environment, T_1 , T_2 , the saturation efficiency, and the amplitude and duration of the saturation pulse. These effects can be incorporated into a general solution obtainable from the analysis of a two-site exchange model in the presence of RF saturation ^{18,19}. As $\Delta\omega$ increases linearly with static field strength, CEST imaging greatly benefits from ultra-high magnetic fields. As a result, molecules with high exchange rates, which do not satisfy the condition in eq. (1) at lower fields ($\leq 3T$), may still demonstrate a CEST effect at 7T. While the chemical shift difference is directly related to the magnetic field strength, the chemical exchange rate depends mainly on the exchange type and environment. *In vivo*, the exchange rate is highly sensitive to changes in tissue pH²⁰. The chemical exchange rate can change by several orders of magnitude with changes in pH as small as 1 unit. It is therefore

critical to identify endogenous agents whose chemical exchange rates satisfy Eq. (1) under physiological conditions.

Technical Considerations: The CEST effect depends on several factors such as field strength (B_0), concentration of metabolite with exchanging spins, exchange rate, temperature, static magnetic field (B_0) and RF field (B_1) inhomogeneities, T_1 of water protons, RF saturation pulse duration and amplitude. Thus in measuring the CEST effect from a given metabolite all these factors have to be optimized and accounted for.

B_0 and B_1 field homogeneities present a challenge for CEST imaging. This is particularly significant at ultra-high magnetic fields, where the effects of these inhomogeneities are magnified¹³. B_0 field inhomogeneities lead to a shift in the water resonance frequency that results in asymmetric direct water saturation effects and as a result artificial CEST effects in asymmetry analysis. B_1 inhomogeneity on the other hand results an increase or decrease in the applied RF. This leads to either a reduction of saturation efficiency or an increase in direct water saturation effects, which will create inaccuracies in the CEST asymmetry maps. Several methods have been developed for correction of B_0 and B_1 inhomogeneities²¹⁻²³.

In general, low power long duration rectangular saturation pulses are employed in phantom and animal model studies. However, due to clinical scanner limitations, trains of Gaussian or Hanning windowed short duration pulses separated by short delays are employed²⁴. Currently, most applications of CEST (specifically, amine and $-OH$) utilize single slice readout. CEST requires acquisition at multiple saturation frequencies with long repetition times (TR) to allow for relaxation. To address this issue, new multi-slice and three dimensional (3D) acquisition techniques have emerged.^{25,26} All of these methods rely on steady state CEST contrast and as a result may not be optimal for faster exchanging spins. Development of faster, multi-slice or 3D CEST techniques is important to translating amine and $-OH$ CEST imaging to more clinical applications. In order to address many confounders of the CEST effects including NOE effects and MTR asymmetry several methods have also been developed that utilize z-spectral fitting for computing the CEST effect²⁷. While these methods show promise for decoupling the confounding contributions to the CEST effect, further work is necessary to assess their *in vivo* accuracy.

Results and Discussion: CEST applications in cancer imaging

Many of the metabolites originally examined for use as exogenous contrast agents are found endogenously at concentrations high enough for detection¹⁶. The feasibility of endogenous CEST imaging was first demonstrated in imaging of urea in the bladder of healthy human subjects⁴. Since then, several endogenous metabolites with exchangeable protons (amide ($-NH$), amine ($-NH_2$) and hydroxyl ($-OH$) groups) with optimal exchange properties under physiological conditions have been identified and imaged *in vivo*¹².

Amide Proton ($-NH$) Transfer (APT): Imaging of Changes in Protein Content and pH in Tumors

The CEST effects from amide protons were first demonstrated in the rat brain at 4.7T, and this method was referred to as amide proton transfer (APT)²⁸. Amide protons have a chemical shift 3.5 ppm down field from water, which corresponds to the amide resonance at about 8.3 ppm in the NMR spectrum²³. Additionally, due to their very slow exchange rate ($\sim 30 \text{ s}^{-1}$)²⁹, it is possible to obtain almost complete saturation using a low power, long duration saturation pulse and these experiments can be performed at 3T as well as at higher fields. APT imaging has been utilized in a range of applications including studies in 9L gliosarcoma tumor rat models, human brain tumors^{23,26,30-32}, breast cancer³³⁻³⁵, prostate and bladder cancer³⁶, as well as others, where an increase in APT in tumor regions was observed. This increase was hypothesized to be due

to increased amide proton content in the brain tumors and or due to pH changes. More recent studies have demonstrated the feasibility of APT imaging for tumor grading^{37,38}, which was further extended to studies of radiation necrosis. APT could differentiate between active orthotopic gliomas that appear hyperintense from radiation necrosis, which appears hypointense³⁹.

APT imaging contrast originates from a combination of changes in protein content (hence –NH) and pH¹³ of the tissue. In addition, APT measurement is affected by MT asymmetry and nuclear Overhauser effect (NOE). Therefore, to realize the full potential of APT, methods need to be developed to remove confounding effects such as MT asymmetry and NOE. Nonetheless, the slow exchange rate and relatively high concentrations of amide protons create conditions, which potentially allow this technique to be translated to clinical applications as an “index” of molecular changes.

Hydroxyl (-OH) CEST: Imaging of Glucose Metabolism in Tumors

Another important application of CEST imaging is in studying exchange of –OH groups in metabolites such as, Glycogen, GAG, MI and Glucose. Recently, -OH groups of glucose have been exploited in imaging glucose in phantoms as well as in *in vivo* systems (GlucoCEST)⁴⁰⁻⁴³. Tumors typically rely more on anaerobic glycolytic metabolism than normal tissues, due to hypoxia or inhibited mitochondrial function, a phenomenon widely known as the Warburg effect. As a result, up regulated glucose metabolism is commonly used to detect and characterize tumors with ¹⁸F labeled 2-fluoro-2-deoxy-D-glucose (FDG) PET. Similarly, preferential uptake of injected D-glucose in tumors can be imaged with GlucoCEST.

Recently GlucoCEST has been shown to be sensitive to tumor glucose accumulation in colorectal tumor models and can distinguish tumor types with differing metabolic characteristics and pathophysiology⁴³. In another study, significant GlucoCEST signal enhancement has been shown at 11.7T in mice in two human breast cancer cell lines during systemic sugar infusion⁴². While more studies are required to understand the clear origin of the observed CEST signal these results show the potential of cancer detection and characterization with MRI using the GlucoCEST effect from simple non-toxic sugars. In addition, feasibility CEST-MRI of two glucose analogs 2-deoxy-D-glucose (2-DG) and FDG has been demonstrated both in phantoms and on mice bearing orthotopic mammary tumors injected with 2-DG or FDG⁴⁴. The tumor exhibited an enhanced CEST effect that persisted for over one hour. These studies show the potential of studying tumor metabolism without using the radiolabeled isotopes.

In general, -OH groups of many metabolites, such as the one described above, resonate at around 1 ppm (0.6 to 1.5 ppm) down field from water and have exchange rates in the range of 500-1500 s⁻¹. These exchange rates typically do not satisfy the condition of slow to intermediate exchange (eq. (1)) on the NMR time scale at lower fields such as 1.5T and 3T. In addition, lower frequency separation from water and the requirement of relatively high saturation power lead to huge direct saturation effects that decrease the sensitivity of CEST. However, as described above, these studies can be performed at higher fields (≥ 7T) with improved sensitivity and have been demonstrated in preclinically relevant applications.

Amine (-NH₂) CEST: Imaging of Protease Activity in Tumors

Amine protons from free amino acids or protein and peptide side chains are another important class of endogenous CEST agents. Endogenous metabolites with exchangeable amine group protons and exchange rates suitable for CEST imaging include glutamate (Glu)²⁴ and Creatine (Cr)⁴⁵. Glu is the major excitatory neurotransmitter in the central nervous system (CNS). Glu exhibits a pH and concentration dependent CEST effect (GluCEST) between its amine group, observed at ~3.0 ppm downfield from water, and bulk water²⁴. Its exchange rate is in the range of 2000 to 6000 s⁻¹. Intravenous Glu injected in a rat brain tumor model with a compromised

blood brain barrier led to an elevation of $\text{GluCEST}_{\text{asym}}$ around the tumor while no changes were seen in the normal appearing tissue.

Cathepsins, cysteine family proteases, are over expressed in many tumors and have been shown to have diagnostic and prognostic value in several types of cancers⁴⁶. Recently it was demonstrated that GluCEST can be used to measure the release of glutamate moieties from cathepsin mediated cleavage of poly-L-glutamate in both *in vitro* and *in vivo* tumor models⁴⁷. Another study has used the GluCEST to monitor the release of glutamate induced by carboxypeptidase G2 (CPG2), an enzyme utilized in cancer gene therapy, in CPG2-expressing cancer cells and purified solution of CPG2⁴⁸. These studies demonstrate the potential of GluCEST method in assessing protease activity in tumors and CPG2-based gene therapy *in vivo*.

Compared to amide, amine protons tend to have faster exchange rates. While this allows for higher saturation transfer efficiency, higher B_1 amplitude is required in order to achieve saturation, which increases direct water saturation effects. Typically, the faster exchange rates of amine protons do not satisfy the slow to intermediate exchange condition (eq. (1)) at low fields ($\leq 3T$) and as a result, amine CEST studies have to be performed at ultrahigh fields ($\geq 7T$).

CEST Imaging of pH: pH is an important marker of many disease processes and pathologies including cancer and stroke. The direct effect of pH on chemical exchange rate makes CEST an ideal technique to assess change in pH *in vivo* with high spatial resolution. As a result, CEST imaging has been used to study and attempt to quantify changes in pH⁴⁹⁻⁵¹. CEST based pH quantification has its own challenges. CEST contrast depends on several parameters including labile proton concentration, temperature, water content, the T_1 of water, saturation parameters as well as any other factors, which affect the chemical environment of the exchanging protons. This makes *in vivo* pH quantification significantly more challenging, as accounting for all of these factors *in vivo* is rather difficult. An alternate strategy is to use a CEST agent with two exchanging sites, which can be used as an internal reference to control for many of these confounds. By using a CEST agent with two exchange sites, the ratio of the CEST asymmetry at each exchange site will vary with the ratio of exchange rates, and can thus be used for pH calibration⁵¹. However, this technique was only validated *in vitro* and has not been applied to *in vivo* endogenous pH measurement studies.

In addition to the conventional method of measuring $\text{CEST}_{\text{asym}}$ described by equation (2), several other methods have been developed for exchange transfer MRI. These include frequency-labeled exchange transfer (FLEX)⁵², CESTrho⁵³, length and offset varied saturation (LOVARS)⁵⁴, two-frequency RF irradiation⁵⁵, chemical exchange rotation transfer (CERT)⁵⁶ as well as others. These methods may further advance exchange based MRI, but need further characterization in *in vivo* applications.

Conclusions

CEST applications show promise to use MRI as a non-invasive, non-ionizing tool for molecular imaging of cancers. Several studies have demonstrated the feasibility of implementing these methods both in preclinical tumor models as well as in preliminary human studies. These methods can be exploited as quantitative imaging biomarkers for diagnosis and characterization of different types of cancer, as well as in treatment monitoring. Further developments in improving the acquisition speed, spatial coverage, and techniques to enhance the specificity of the methods will enable widespread translation of CEST MRI into the clinical setting.

Acknowledgements: This work was supported by a NIBIB supported resources center grants P41-EB015893, P41-EB015893-S1 and NIH grants 1R21-DA032256-01 and T32EB009384.

References

1. Forsen, S. & Hoffman, R.A. Study of moderately rapid chemical exchange reactions by means of nuclear magnetic double resonance. *J. Chem. Phys.* **39**, 2892-2901 (1963).
2. Gutowsky, H.S. Disociation, chemical exchange, and the proton magnetic resonance in some aqueous electrolytes. *J. Chem. Phys.* **21**, 1688-1694 (1953).
3. Wolff, S.D. & Balaban, R.S. NMR imaging of labile proton-exchange. *J. Magn. Reson.* **86**, 164-169 (1990).
4. Dagher, A.P., Aletras, A., Choyke, P. & Balaban, R.S. Imaging of urea using chemical exchange-dependent saturation transfer at 1.5T. *J Magn Reson Imaging* **12**, 745-748 (2000).
5. Guivel-Scharen, V., Sinnwell, T., Wolff, S.D. & Balaban, R.S. Detection of proton chemical exchange between metabolites and water in biological tissues. *J Magn Reson* **133**, 36-45 (1998).
6. Aime, S., *et al.* High-sensitivity lanthanide (III) based probes for MR-medical imaging. *Coordination Chemistry Reviews* **250**, 1562-1579 (2006).
7. Woods, M., Woessner, D.E. & Sherry, A.D. Paramagnetic lanthanide complexes as PARACEST agents for medical imaging. *Chemical Society reviews* **35**, 500-511 (2006).
8. Zhang, S., Merritt, M., Woessner, D.E., Lenkinski, R.E. & Sherry, A.D. PARACEST agents: modulating MRI contrast via water proton exchange. *Accounts of chemical research* **36**, 783-790 (2003).
9. Hancu, I., *et al.* CEST and PARACEST MR contrast agents. *Acta Radiol* **51**, 910-923 (2010).
10. Sherry, A.D. & Woods, M. Chemical exchange saturation transfer contrast agents for magnetic resonance imaging. *Annu Rev Biomed Eng* **10**, 391-411 (2008).
11. Terreno, E., Castelli, D.D. & Aime, S. Encoding the frequency dependence in MRI contrast media: the emerging class of CEST agents. *Contrast media & molecular imaging* **5**, 78-98 (2010).
12. Kogan, F., Hariharan, H. & Reddy, R. Chemical Exchange Saturation Transfer (CEST) Imaging: Description of Technique and Potential Clinical Applications. *Current radiology reports* **1**, 102-114 (2013).
13. van Zijl, P.C. & Yadav, N.N. Chemical exchange saturation transfer (CEST): what is in a name and what isn't? *Magn Reson Med* **65**, 927-948 (2011).
14. Vinogradov, E., Sherry, A.D. & Lenkinski, R.E. CEST: from basic principles to applications, challenges and opportunities. *J Magn Reson* **229**, 155-172 (2013).
15. Zhou, J. & van Zijl, P.C. Chemical exchange saturation transfer imaging and spectroscopy. *Prog. NMR Spectrosc* **48**, 109-136 (2006).
16. Ward, K.M., Aletras, A.H. & Balaban, R.S. A new class of contrast agents for MRI based on proton chemical exchange dependent saturation transfer (CEST). *J Magn Reson* **143**, 79-87 (2000).
17. Liu, G., Gilad, A.A., Bulte, J.W., van Zijl, P.C. & McMahon, M.T. High-throughput screening of chemical exchange saturation transfer MR contrast agents. *Contrast media & molecular imaging* **5**, 162-170 (2010).
18. Sun, P.Z., van Zijl, P.C. & Zhou, J. Optimization of the irradiation power in chemical exchange dependent saturation transfer experiments. *J Magn Reson* **175**, 193-200 (2005).
19. Woessner, D.E., Zhang, S., Merritt, M.E. & Sherry, A.D. Numerical solution of the Bloch equations provides insights into the optimum design of PARACEST agents for MRI. *Magn Reson Med* **53**, 790-799 (2005).
20. Liepinsh, E. & Otting, G. Proton exchange rates from amino acid side chains--implications for image contrast. *Magn Reson Med* **35**, 30-42 (1996).

21. Kim, M., Gillen, J., Landman, B.A., Zhou, J. & van Zijl, P.C. Water saturation shift referencing (WASSR) for chemical exchange saturation transfer (CEST) experiments. *Magn Reson Med* **61**, 1441-1450 (2009).
22. Singh, A., Cai, K., Haris, M., Hariharan, H. & Reddy, R. On B(1) inhomogeneity correction of in vivo human brain glutamate chemical exchange saturation transfer contrast at 7T. *Magn Reson Med* (2012).
23. Zhou, J., Lal, B., Wilson, D.A., Laterra, J. & van Zijl, P.C. Amide proton transfer (APT) contrast for imaging of brain tumors. *Magn Reson Med* **50**, 1120-1126 (2003).
24. Cai, K., *et al.* Magnetic resonance imaging of glutamate. *Nat Med* **18**, 302-306 (2012).
25. Jones, C.K., *et al.* In vivo three-dimensional whole-brain pulsed steady-state chemical exchange saturation transfer at 7 T. *Magn Reson Med* **67**, 1579-1589 (2012).
26. Zhou, J., *et al.* Three-dimensional amide proton transfer MR imaging of gliomas: Initial experience and comparison with gadolinium enhancement. *J Magn Reson Imaging* **38**, 1119-1128 (2013).
27. Zaiss, M., Schmitt, B. & Bachert, P. Quantitative separation of CEST effect from magnetization transfer and spillover effects by Lorentzian-line-fit analysis of z-spectra. *J Magn Reson* **211**, 149-155 (2011).
28. Zhou, J., Payen, J.F., Wilson, D.A., Traystman, R.J. & van Zijl, P.C. Using the amide proton signals of intracellular proteins and peptides to detect pH effects in MRI. *Nat Med* **9**, 1085-1090 (2003).
29. Zhou, J., Wilson, D.A., Sun, P.Z., Klaus, J.A. & Van Zijl, P.C. Quantitative description of proton exchange processes between water and endogenous and exogenous agents for WEX, CEST, and APT experiments. *Magn Reson Med* **51**, 945-952 (2004).
30. Hong, X., *et al.* Quantitative multiparametric MRI assessment of glioma response to radiotherapy in a rat model. *Neuro Oncol* (2013).
31. Togao, O., *et al.* Amide proton transfer imaging of adult diffuse gliomas: correlation with histopathological grades. *Neuro Oncol* (2013).
32. Zhou, J., Hong, X., Zhao, X., Gao, J.H. & Yuan, J. APT-weighted and NOE-weighted image contrasts in glioma with different RF saturation powers based on magnetization transfer ratio asymmetry analyses. *Magn Reson Med* **70**, 320-327 (2013).
33. Schmitt, B., *et al.* A new contrast in MR mammography by means of chemical exchange saturation transfer (CEST) imaging at 3 Tesla: preliminary results. *Rofo* **183**, 1030-1036 (2011).
34. Klomp, D.W., *et al.* Amide proton transfer imaging of the human breast at 7T: development and reproducibility. *NMR Biomed* **26**, 1271-1277 (2013).
35. Dula, A.N., *et al.* Amide proton transfer imaging of the breast at 3 T: establishing reproducibility and possible feasibility assessing chemotherapy response. *Magn Reson Med* **70**, 216-224 (2013).
36. Jia, G., *et al.* Amide proton transfer MR imaging of prostate cancer: a preliminary study. *J Magn Reson Imaging* **33**, 647-654 (2011).
37. Wen, Z., *et al.* MR imaging of high-grade brain tumors using endogenous protein and peptide-based contrast. *Neuroimage* **51**, 616-622 (2010).
38. Zhou, J., *et al.* Practical data acquisition method for human brain tumor amide proton transfer (APT) imaging. *Magn Reson Med* **60**, 842-849 (2008).
39. Zhou, J., *et al.* Differentiation between glioma and radiation necrosis using molecular magnetic resonance imaging of endogenous proteins and peptides. *Nat Med* **17**, 130-134 (2011).
40. van Zijl, P.C., Jones, C.K., Ren, J., Malloy, C.R. & Sherry, A.D. MRI detection of glycogen in vivo by using chemical exchange saturation transfer imaging (glycoCEST). *Proc Natl Acad Sci U S A* **104**, 4359-4364 (2007).

41. Chilakapati, S., *et al.* Characterization of CEST effect from Glucose In Vitro. in *International Society of Magnetic Resonance in Medicine* 2335 (Melbourne, Australia, 2012).
42. Chan, K.W., *et al.* Natural D-glucose as a biodegradable MRI contrast agent for detecting cancer. *Magn Reson Med* **68**, 1764-1773 (2012).
43. Walker-Samuel, S., *et al.* In vivo imaging of glucose uptake and metabolism in tumors. *Nat Med* **19**, 1067-1072 (2013).
44. Rivlin, M., Horev, J., Tsarfaty, I. & Navon, G. Molecular imaging of tumors and metastases using chemical exchange saturation transfer (CEST) MRI. *Scientific reports* **3**, 3045 (2013).
45. Kogan, F., *et al.* Method for high-resolution imaging of creatine in vivo using chemical exchange saturation transfer. *Magn Reson Med* (2013).
46. Berdowska, I. Cysteine proteases as disease markers. *Clinica chimica acta; international journal of clinical chemistry* **342**, 41-69 (2004).
47. Haris, M., *et al.* GluCEST Imaging of Tumor Protease Activity. in *International Society of Magnetic Resonance in Medicine* (submitted) (Milan, Italy, 2104).
48. Jamin, Y., Eykyn, T.R., Poon, E., Springer, C.J. & Robinson, S.P. Detection of the Prodrug-Activating Enzyme Carboxypeptidase G2 Activity with Chemical Exchange Saturation Transfer Magnetic Resonance. *Molecular imaging and biology : MIB : the official publication of the Academy of Molecular Imaging* (2013).
49. Sun, P.Z., Benner, T., Kumar, A. & Sorensen, A.G. Investigation of optimizing and translating pH-sensitive pulsed-chemical exchange saturation transfer (CEST) imaging to a 3T clinical scanner. *Magn Reson Med* **60**, 834-841 (2008).
50. Sun, P.Z. & Sorensen, A.G. Imaging pH using the chemical exchange saturation transfer (CEST) MRI: Correction of concomitant RF irradiation effects to quantify CEST MRI for chemical exchange rate and pH. *Magn Reson Med* **60**, 390-397 (2008).
51. Ward, K.M. & Balaban, R.S. Determination of pH using water protons and chemical exchange dependent saturation transfer (CEST). *Magn Reson Med* **44**, 799-802 (2000).
52. Yadav, N.N., *et al.* Detection of rapidly exchanging compounds using on-resonance frequency-labeled exchange (FLEX) transfer. *Magn Reson Med* **68**, 1048-1055 (2012).
53. Kogan, F., *et al.* Investigation of chemical exchange at intermediate exchange rates using a combination of chemical exchange saturation transfer (CEST) and spin-locking methods (CESTRho). *Magn Reson Med* (2011).
54. Song, X., *et al.* CEST phase mapping using a length and offset varied saturation (LOVARS) scheme. *Magn Reson Med* **68**, 1074-1086 (2012).
55. Lee, J.S., Regatte, R.R. & Jerschow, A. Isolating chemical exchange saturation transfer contrast from magnetization transfer asymmetry under two-frequency rf irradiation. *J Magn Reson* **215**, 56-63 (2012).
56. Zu, Z., *et al.* A new method for detecting exchanging amide protons using chemical exchange rotation transfer. *Magn Reson Med* **69**, 637-647 (2013).